Immunosensors Made of Polymer-Infused Porous Paper for the Non-Invasive Detection of Airways Cytokines Trapped by Porous Face Masks

Andreu Vaquer,[1,2,ǂ] Cristina Adrover-Jaume,[1,2,ǂ] Antonio Clemente,[1,*] Amanda Iglesias,[3,4] Meritxell López,[3,4,5,#] Rocío Martínez,[3,5,#] Isabel M Roig,[5,#] Borja G Cosío,[3,4,5] and Roberto de la Rica.[1,6,*]

[1]Multidisciplinary Sepsis Group, Hospital Universitario Son Espases, Health Research Institute of Balearic Islands (IdISBa), Palma de Mallorca, Spain

[2]Department of Chemistry, University of the Balearic Islands, Palma de Mallorca, Spain

[3]Inflamación, reparación y cáncer en enfermedades respiratorias (i-RESPIRE), Hospital Universitario Son Espases, Health Research Institute of Balearic Islands (IdISBa), Palma de Mallorca, Spain

[4]CIBER de Enfermedades Respiratorias (CIBERES), Instituto de Salud Carlos III, Madrid, Spain

[5]Department of Respiratory Medicine, Hospital Universitario Son Espases, Palma de Mallorca, Spain

[6]CIBER de Enfermedades Infecciosas (CIBERINFEC), Instituto de Salud Carlos III Madrid, Spain

[ǂ]Contributed equally.

[#]Contributed equally.

*Corresponding authors: tonydelaricalab@gmail.com, roberto.delarica@ssib.es

ABSTRACT

The diverse physicochemical properties of polymers make them perfect candidates for developing biosensor elements when combined with porous substrates. For example, microfluidic channels, valves, reservoirs and biorecognition elements have been proposed that rely on filling the cavities of porous cellulose with different polymers. Yet, highly concentrated polymers are often too viscous to dispense them with precision using conventional printing methods. This increases the manufacturing variability, which degrades the performance of the biosensors. Here this issue is solved with a new method for infusing porous materials (filter paper) with concentrated polymers (PSS) that circumvents the dropwise addition of highly viscous reagents. The resulting films contain homogenously distributed polymers, which reduces the intra- and inter-batch variabilities of biosensors based on dispensing nanoparticles from the reservoirs. The proposed method was utilized to develop immunosensors for detecting the cytokines IL-6 and IL-5 in aerosols, which were trapped by the polypropylene layer of a surgical face mask (limit of detection 10^{-2} pg·mL^{-1}). Using this approach, we were able to detect elevated levels of airways cytokines when exacerbated COPD patients and eosinophilic asthma patients wore the face mask for 30 minutes. The results shown here pave the way for upscaling the manufacturing of paper-based nanoparticle biosensors, which is a crucial step towards their future commercialization.

Keywords: breath, paper-based, biosensor, COPD, asthma, cytokine

INTRODUCTION

Three-dimensional porous materials have become a central component of the biosensor development toolbox thanks to the unique properties bestowed by their hollow structure[1,2]. For example, materials with different pore dimensions can be used to separate particles according to size[3,4], or to wick liquids in microfluidic devices[5,6]. The porous scaffold can also be filled with polymers with different functions, which has been leveraged for fabricating microfluidic channels[7,8], valves[6,9,10], reservoirs[11–13], and recognition elements[14,15]. For instance, cellulose can be modified with water-soluble polymers in order to obtain reservoirs that store reagents in dry conditions during extended periods of time[16,17]. The reservoirs are fabricated by dispensing a drop of polymer onto filter paper, which prevents the irreversible adsorption of stored reagents to the cellulose scaffold. The reservoir is then filled with enzymes or nanoparticles by adding a drop of the reagent on top of the dried polymer[18]. This manufacturing method is prone to high variability because concentrated polymers are very viscous, which makes it difficult to dispense them dropwise with high precision. Furthermore, it is also hard to control the drying process, which often results in more concentrated solutes at the rim than in the center of the drop (i.e. a "coffee ring")[19,20]. These issues compromise the performance of biosensors fabricated using paper reservoirs, since the manufacturing variability translates into analytical imprecision.

Herein, a new manufacturing method is proposed for developing paper-based reservoirs with lower intra- and inter-batch variability. It consists of substituting the dropwise addition of polymers for the generation of a polymer film that infuses the whole paper sheet (Figures 1A-1B). Whereas previous publications relied on dispensing small drops of highly viscous polymer to prepare reservoirs, here we report for the first time that whole paper sheets can be modified with the polymer for the upscaled production of biosensors with improved inter-batch variability. Furthermore, polymer films are dried under controlled conditions, which results in a homogenous distribution throughout the cellulose scaffold that prevents the formation of coffee rings. This, in turn, reduces the intra-batch variability of biosensors fabricated this way. The resulting polymer-infused paper reservoirs were used to store antibody-decorated nanoparticles aimed at detecting the cytokines IL-6 and IL-5, which are inflammation biomarkers, in aerosols (Figure 1C). It has been shown that cytokines are present in condensed exhaled breath[21,22], thus paving the way for characterizing inflammatory processes in the airways through the

detection of these biomarkers in the aerosols produced when breathing. Here we implement another porous material, the nonwoven polypropylene layer of a surgical face mask, to capture the biomarkers (Figure 1C). In this approach, aerosols produced as the patient breaths are trapped by the hydrophobic polypropylene mesh, which renders the cytokines adsorbed to the porous material. The biomarkers are then specifically detected by pressing the reservoirs against the face mask. This transfers antibody-nanoparticles and generates colored dots whose pixel intensity is related to the concentration of the cytokine in exhaled breath. Using this approach, we were able to detect elevated levels of airway cytokines when exacerbated COPD patients and eosinophilic asthma patients wore the face mask for 30 minutes. Mask analysis was completed in less than 10 min using a smartphone app for colorimetric signal quantification, yielding a total turnaround time from sample collection to biomarker detection within 40 min (Figure 1C). The ability of sampling the airways non-invasively with a face mask and detecting cytokines with the proposed immunosensors could revolutionize the management of inflammatory airways diseases, which urgently need new point-of-care methods for guiding their diagnosis and treatment.

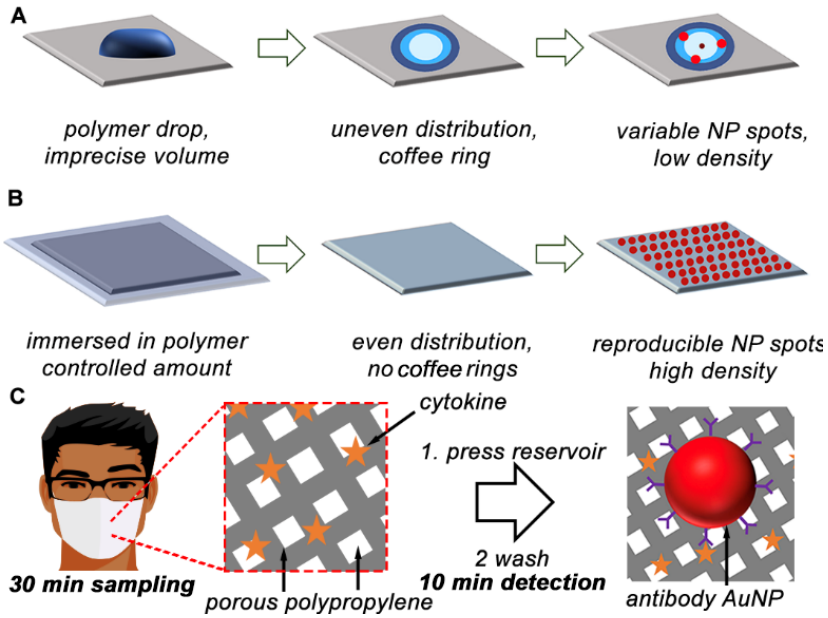

Figure 1. Schematic representation of methods for manufacturing reservoirs (A-B) and immunosensors (C) for detecting airway cytokines; (A) adding the polymer as drops is difficult because it requires dispensing small volumes of a highly viscous reagent, which, upon drying generates coffee rings; (B) immersing the porous substrate in the polymer enables a better control over the amount of polymer and results in a homogenous film upon drying; (C) Polymer reservoirs were filled with antibody-decorated gold nanoparticles (antibody AuNPs) and used to detect airway cytokines adhered to a face mask worn by AECOPD or eosinophilic asthma patients.

EXPERIMENTAL SECTION

Functionalization and characterization of antibody-decorated gold nanoparticles

A previously described citrate-reducing method was used to obtain gold nanoparticles (AuNPs) with a diameter of ca. 40 nm[23]. AuNPs were functionalized with specific antibodies by following covalent or physical adsorption protocols for nanoprobes against IL-6 and IL-5, respectively. Reagents used for the synthesis and functionalization of gold nanoparticles can be found in Section S1 in the Supporting information.

Covalent functionalization: Nanoprobes against IL-6 were decorated with antibodies by adapting a published protocol for covalent functionalization. In brief, the citrate around the nanoparticles was substituted for thiol-PEG-acid. After concentration of nanoprobes 250 times via centrifugation, the carboxylic groups were transformed into reactive sulfo-NHS esters via the addition of EDC (1 mg) and sulfo-NHS (2 mg) in 0.5 M MES buffer pH 5.5 for 30 min. Then 200 µL of the nanoprobes was centrifuged at 8000 rpm for 8 min and rabbit anti-IL-6 polyclonal antibody or IgG from rabbit serum (0.75 $mg \cdot mL^{-1}$) was added overnight. Then 200 µL of a blocking solution containing glycine (0.1 M) and BSA (10 $mg \cdot mL^{-1}$) in phosphate buffer (0.1 M, pH 7.0) was added and incubated for 30 min for capping any free sulfo-NHS ester group. Subsequently, nanoparticles were washed 5 times with PBST (7000 rpm, 7 min). Finally, the pellet was resuspended in 200 µL PBST.

Functionalization by physical adsorption: Nanoprobes against IL-5 were modified with antibodies following an adapted protocol for functionalization by physical adsorption. In brief, 200 µl of IgG from rabbit serum or rabbit anti-IL-5 polyclonal antibody (both at 40 $\mu L \cdot mL^{-1}$) was added to 2 mL of gold nanoparticles (AuNPs) and incubated for 20 min under vigorous stirring. Then, the coated AuNPs were blocked by adding 200 µL of 10 $mg \cdot mL^{-1}$ BSA solution (in water) for 20 min at RT. Finally, Ab-AuNPs were centrifuged at 6000 rpm for 7 min and the resulting pellet was resuspended in 100 µl of capping solution with 50 $mg \cdot mL^{-1}$ sucrose and 1 $mg \cdot mL^{-1}$ BSA, previously prepared in water. The functionalized AuNPs were stored at 4 ºC until use.

Characterization of functionalized gold nanoparticles: Nanoparticle size was studied by nanoparticle tracking analysis (NTA) with a NanoSight NS 300 equipment. Measurements of Z potential were made with Marlvern Zetasizer Nano-ZS90. Size and Z potential of nanoparticles were measured in all different steps of the functionalization.

Fabrication of paper reservoirs

Section S2 in the Supporting information shows experiments performed to optimize the concentration of PSS for the fabrication of reservoirs using the polymer-infusing or the dropwise method. Polymer-infused reservoirs were obtained with the following procedure. Whatman filter paper #1 was cut into 9 x 9 cm^2 squares. Then, 1 mL of 18% PSS was added to a petri dish and the paper square was placed above the liquid. Afterwards, 2 mL of 18% PSS was added above the paper square. Finally, to obtain the film, the petri dish containing the piece of paper was dried in an oven for 20-25 min at 37 ºC. To make reservoirs with polymer drops, 5 µL of 30% PSS was added in the center of a 1.5 x 1.5 cm^2 piece of Whatman filter paper #1 and let dry at RT. To fill the reservoirs with nanoparticles, 0.5 µL of antibody-decorated AuNPs was dispensed onto the PSS film using a Hamilton syringe coupled to a microdrop dispenser.

To measure the intra- and inter-batch variability in the colorimetric signal, avidin-decorated AuNPs were used to detect biotinylated BSA as a model ligand-receptor interaction. To this end, Whatman filter paper #1 was modified with 10 µL of 30 $\mu g \cdot mL^{-1}$ biotinylated BSA. Control experiments were performed with BSA. Upon drying at RT, 1 mL of PBS-BSA was added to block the paper. Avidin-AuNPs were then dispensed by pressing the reservoirs against the receiving paper substrates for 5 min. After washing 5 times the paper substrates were scanned with a Brother MFC-1910W scanner and the pixel intensity was measured with ImageJ software. The colorimetric signal S is the integer obtained after subtracting the pixel intensity of the background in the gray channel.

Detection of cytokines attached to face masks

IL-6 and IL-5 solutions in the range from 0.01 to 1000 $pg \cdot mL^{-1}$ were prepared in PBS. The solutions were transferred to a spray bottle. The spray bottle and a piece of 1.5cm x 2 cm surgical face mask were held by a 3D printed device that maintained a fixed distance between them (Section S3 in the Supporting information). The solution containing the protein was sprayed twice at a fixed distance of 5 cm. The polypropylene layer was separated after drying at RT. Subsequently, the layer was hydrated and blocked with 1 mL of PBS-BSA, and the polymer-infused paper reservoir was pressed against it for 5 min. Then, the reservoir was removed, and the polypropylene layer was washed with 1

mL of PBST. The colorimetric signal was measured with a mobile app for smartphone-based densitometry described in previous publications[24].

Detection of cytokines in face masks worn by patients

15 COPD patients with acute exacerbation (AECOPD) and 11 patients with severe eosinophilic asthma (without signs of exacerbation) were included in the IL-6 and IL-5 study, respectively. Exacerbation was defined by an increase of symptoms of dyspnea and change in sputum purulence. All patients used inhaled corticosteroids as regular therapy. Patients that used additional immunomodulatory therapies (oral and systemic corticosteroids or immunosuppressant drugs) within the 2-week period prior recruitment were excluded. All patients with severe eosinophilic asthma were eligible but naïve for biological immunotherapy targeting IL-5/IL-5R axis at recruitment. Patients were asked to wear a surgical face mask for 30 min (lower wearing times decreased the sensitivity of the sensor as shown in Section S4 of the Supporting information). The control group consisted in 10 healthy subjects (with no lung disease) that also wore a face mask for 30 min. The face mask was stored at -20 ºC until it was analyzed. The study was conducted according to the ethical guidelines of the 1975 Declaration of Helsinki. All samples were collected after informed consent from patients or a family member was obtained.

In the face masks collected from patients two 1.5cm × 2cm squares were cut in the center of each one. The hydrophobic polypropylene layer was then isolated and human IL-6 or IL-5 was detected with the method described above.

RESULTS AND DISCUSSION

Figure 2 shows photographs of a paper sheets modified with PSS following the two methods schematized in Figure 1. When the polymer is deposited as drops (5 μL), the liquid expands uncontrollably, which limits the number of nanoparticle reservoirs that can be manufactured in a single paper sheet (Figures 2A-2B). Furthermore, the paper sheet becomes heavily wrinkled and warped when the polymer dries. On the contrary, polymer films fill the entire piece of paper (Figure 2C), and therefore it is possible to increase the number of nanoparticle-filled reservoirs per unit area (Figure 2D). The films

do not warp, which makes it possible to deposit nanoparticles using a microarray dispenser (Section S5 in the Supporting information). This paves the way for filling the reservoirs with antibody-nanoparticles using piezoelectric dispensing methods, which are commonly used in the *in vitro* diagnostics industry[25].

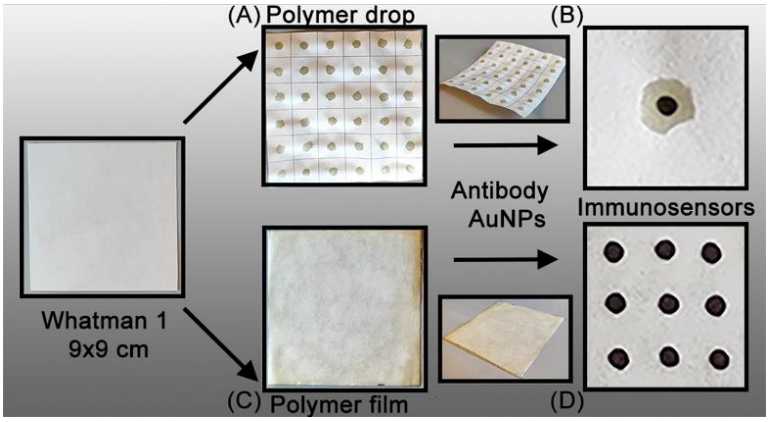

Figure 2. Fabrication of polymer reservoirs for paper immunosensors. Photographs of polymer reservoirs prepared with the drop-casting method (A), or the film-infusing method (B), before and after filling them with burgundy-colored AuNPs.

We then studied the impact of the polymer deposition method on the intra-batch variability. In Figures 3A and 3B, close-up photographs and profile analyses show that, in contrast to reservoirs fabricated using polymer films, polymer drops generate coffee rings upon drying[20,26], that is, the polymer is more concentrated in the periphery than in the center. This means that immunosensors fabricated with polymer drops may perform differently if the nanoparticles are spotted in the center or in the periphery of the polymer drop. In Figure 3C, when the nanoparticles are spotted in the center of the drop (position 1 in Figure 3A) the colorimetric signal generated by the specific recognition of biotin is higher than when the drop is not perfectly centered (positions 2 to 5 in Figure 3A). Conversely, all positions in Figure 3B produce comparable signals when the biosensors are fabricated on paper substrates modified with polymer films (Figure 3D). This means that the intra-batch fabrication variability is higher when manufacturing biosensors using polymer drops than when using polymer films, since a little misalignment between the polymer and nanoparticle drops will produce immunosensors with different analytical performance. Indeed, the standard deviation of immunosensors fabricated using the drop-casting method ranged between 6.66 and 24.01 depending on the alignment between the two processes, whereas in film-based immunosensors it only varied between 0.28 and 6.10.

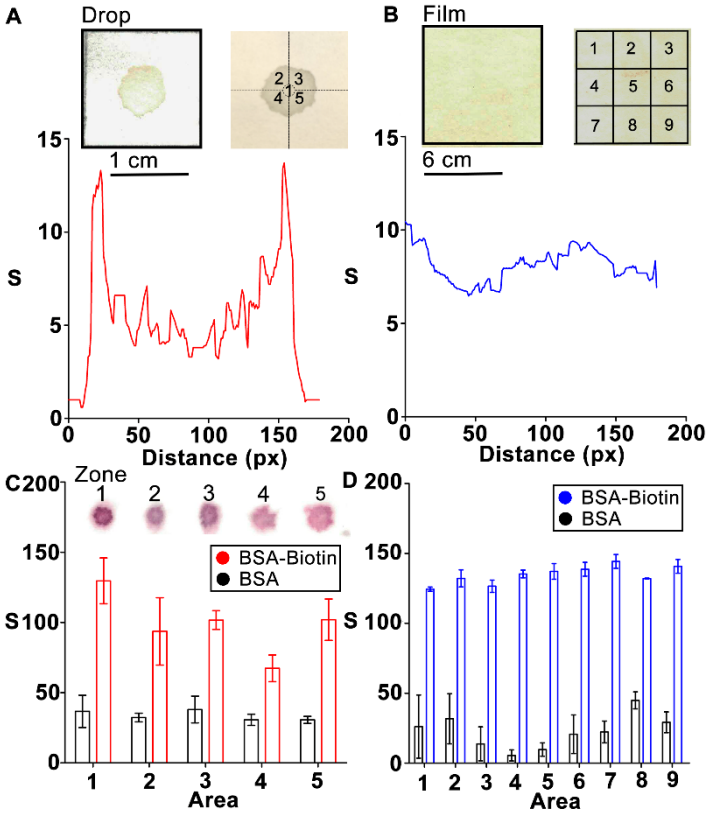

Figure 3. **Analysis of intra-spot and intra-film variability.** Scanned images of paper substrates after imbuing them with PSS drops (30% v/v, (A)) or films (18% v/v, (B)) and profile analysis of images in (A) and (B), respectively. (C) and (D): colorimetric signals for detecting biotin-BSA (red, blue) or control BSA (black) with biosensors prepared spotting nanoparticles in the areas designated in (A) and (B), respectively. Error bars are the standard deviation of 3 independent experiments.

Next, we studied the impact of the polymer deposition method in the inter-batch variability. First, we measured the variability associated to pipetting the viscous polymer by weighing out the drops pipetted with different methods. In Table 1, pipetting 30% PSS increases the standard deviation (SD) and relative standard deviation (RSD) compared to pipetting the same volume of water. Conversely, generating polymers films requires adding higher volumes of PSS at a lower concentration, which can be dispensed with higher precision (lower RSD). Finally, the inter-batch variability of the colorimetric signals generated by the biosensors is also lower when the polymer is deposited as a film than when dispensed as a drop. These results demonstrate that polymer films yield more precise biosensors. Furthermore, this method makes it possible to increase the number of nanoparticle spots within a paper sheet without warping it. This makes polymer films better candidates for the upscaled production of paper immunosensors.

	Polymer weight			Colorimetric signal	
Reagent	Water	30% PSS	18% PSS	30% PSS	18%
Method	drop	drop	film	drop	film
Mean	5.4 mg	6.5 mg	1016.5 mg	93.22	108.19
SD	0.1	1.1	28.7	19.69	9.83
RSD (%)	2.1	17.7	2.8	21	9

Table 1. Intra-batch variability measured as the amount of polymer deposited on the paper (polymer weight), or the colorimetric signal for detecting biotin-BSA with avidin-AuNPs, after preparing different batches (n=15) using different manufacturing methods. SD: standard deviation; RSD: relative standard deviation.

Next we confirmed the correct functionalization of nanoprobes with antibodies against IL-6 and IL-5. Figure 4A demonstrates the covalent functionalization of nanoparticles with α-IL6 or rabbit IgG. In this Figure, the particle size increases from 45 nm in citrate nanoparticles to 52 nm after SH-PEG-COOH addition and 53 nm after modification with antibodies (Figure 4A). Z-potential values mainly change after PEG grafting and remain similar after antibody immobilization (insert in Figure 4A). Figures 4B and 4C show the characterization of nanoparticles functionalized with α-IL5 or rabbit IgG respectively, via physical adsorption. In this case, particle size increases from 42.6 nm (Figures 4B and 4C) to 55.1 nm (α-IL5 modified nanoprobes, Figure 4B) or 50.7 nm (rabbit IgG modified nanoprobes, Figure 4C). The Z-potential significantly increases (less negative) in every step of the modification (inserts in Figures 4B and 4C).

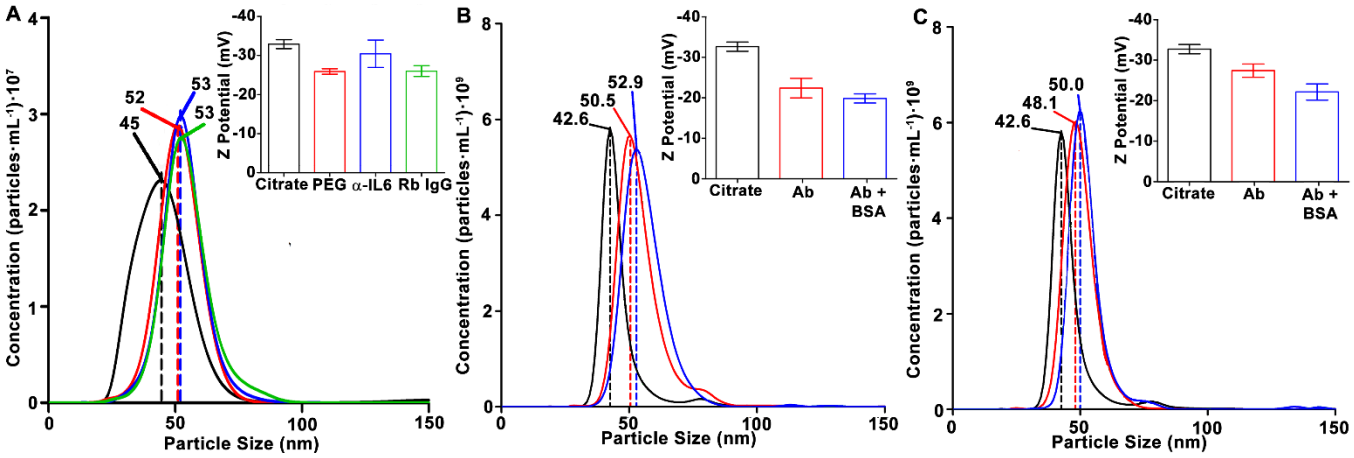

Figure 4. Characterization of functionalized gold nanoparticles. Evaluation of hydrodynamic radius determined by nanoparticle tracking analysis in each step of the functionalization of gold nanoparticles (histograms) and Z potential measurements (inserts). Error bars are the SD of three consecutive measurements. Particle distribution of covalent modified gold nanoparticles with α-IL-6 or IgG from rabbit serum (A), and gold nanoparticles modified via physical adsorption with α-IL-5 (B) and IgG from rabbit serum (C). In panel (A): Citrate stabilized nanoprobes (black), PEG stabilized gold nanoparticles (red), final nanoprobes modified with α-IL-6 (blue) or IgG from rabbit serum (green). In panels (B-C): Citrate stabilized nanoparticles (black), modified with α-IL-5 or rabbit IgG (red), and after blocking with BSA (blue).

After demonstrating that polymer-infused porous substrates improve the biosensors performance and that the nanoprobes are correctly functionalized, we applied the acquired know-how for manufacturing immunosensors against IL-6 and IL-5. Since our final goal is to identify IL-6 and IL-5 biomarkers in exhaled breath, we simulated the generation of aerosols by spraying solutions of the target molecules at different concentrations on face masks. In Figures 5A-5B, the immunosensors produce dose-dependent signals that are higher than control experiments performed with nanoparticles modified with immunoglobulins that do not specifically recognize the target molecules. In both cases, the limit of detection was 10^{-2} pg·mL^{-1} (expressed as the first experiment that yields a signal higher than 3xSD_{blank}). Immunosensors for detecting IL-5 showed lower sensitivity (lower slope of the calibration plot in Figure 5B), which is ascribed to either differences in antibody performance or in the methods used for antibody immobilization (Figure 4). It should be noted that the provided calibration plots are only indicative, since the accumulation of antigens onto the polypropylene layer of the face mask depends on the spray bottle used to create the aerosols, the distance between the bottle and the mask, and the number of times that antigen solutions are sprayed, among others. As such, the assay variability, the limit of detection and the sensitivity will differ depending on the method used to spray the targets. Likewise, in real applications, the sensor performance depends on the time that the patient has worn the mask (Figure S4). Nevertheless, the calibration plots demonstrate that the sensors detect aerosol cytokines specifically and in a dose-dependent manner, which validates them for identifying these targets in exhaled breath.

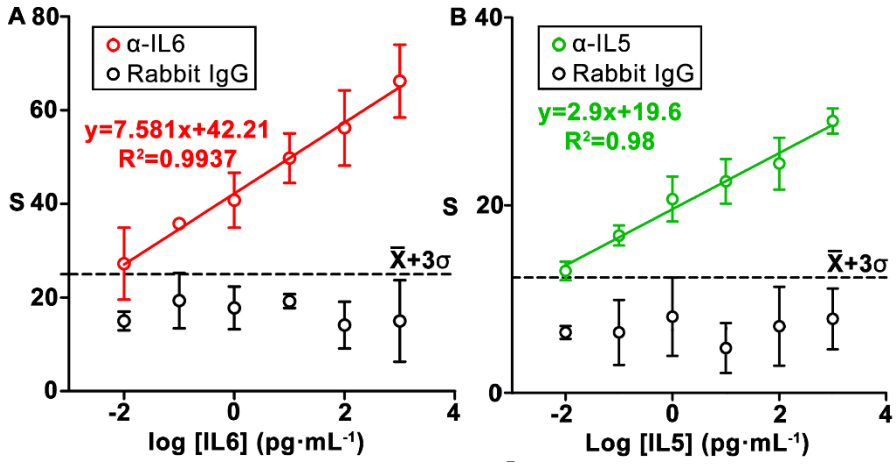

Figure 5. Calibration of immunosensors in face masks sprayed with cytokines. Detection of IL-6 (A) and IL-5 (B) sprayed onto face masks at different concentrations. Control experiments (black dots) were performed with nanoparticles modified with rabbit IgG. Error bars are the standard deviation of 3 independent experiments.

Finally, we investigated the suitability of immunosensors for detecting exhaled IL-6 and IL-5 in face masks worn by AECOPD and eosinophilic asthma patients, respectively. COPD patients suffer episodes of acute worsening of symptoms known as exacerbations that are characterized by higher levels of systemic and/or pulmonary proinflammatory cytokines (e.g. IL-6) [22,27,28]. IL-5 is a key mediator of eosinophil activation pathways in asthma patients[21,29,30]. These observations led us to hypothesize that the proposed biosensors could detected elevated levels of IL-6 and IL-5 in the exhaled breath of these patients. Patients suffering from these respiratory diseases use sanitary resources very frequently and at different levels of healthcare[31]. In this context, we aimed to detect the proposed biomarkers by using a method as user-friendly as possible. For this purpose, the colorimetric signals yielded by immunosensors against IL-6 and IL-5 in face masks worn by patients were measured with a mobile app for smartphone-based densitometry validated in previous publications.[24] In Figure 6, high levels of airway IL-6 are indeed detected in all AECOPD patients (red circles in Figure 6A) compared to healthy controls. Elevated levels of IL-5 were detected in 9 out 11 eosinophilic asthma patients (green circles in Figure 6B).

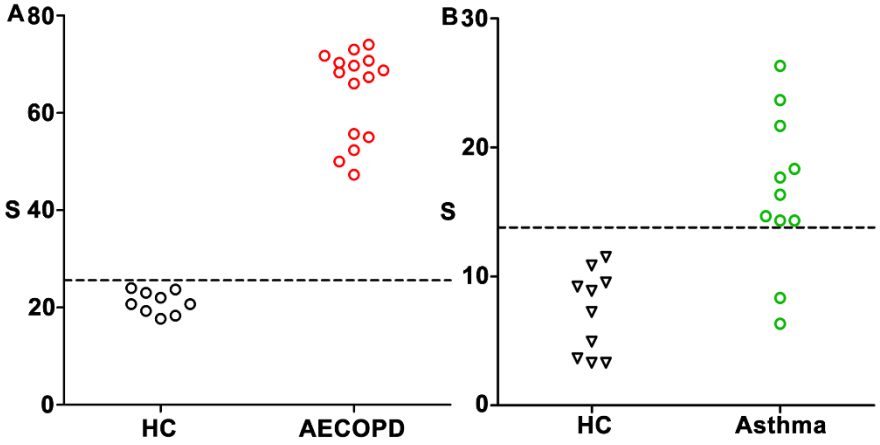

Figure 6. Detection of proinflammatory cytokines in face masks worn by patients with lung diseases. Detection of IL-6 (A) and IL-5 (B) in face masks worn by acute exacerbated COPD patients (AECOPD) and eosinophilic asthma patients, respectively. Horizontal lines represent the mean+2SD of the signals yielded by immunosensors in healthy controls (HC).

Interestingly, Section S6 and Figure S6 of the Supporting information show positive correlations between the signals of immunosensors against airway IL-5 and blood cells counts (neutrophils and eosinophils) in eosinophilic asthma patients. Indeed, the two

patients that yielded undetectable levels of IL-5 also had the lowest levels of circulating neutrophils, which indicates that the immunosensor could not detect the cytokine because they show a reduced inflammation status. Altogether, these results demonstrate that our immunosensors are suitable for the detection of airways IL-6 and IL-5 in patients suffering from inflammatory lung diseases, which are trapped from exhaled air in the face mask worn by the patient.

CONCLUSIONS

In conclusion, we have introduced a new method for infusing filter paper with polymers that reduces the variability when fabricating biosensor reservoirs. This fabrication method renders flat paper reservoirs that can be subsequently filled with antibody-nanoparticles. The resulting paper immunosensors were used to detect IL-6 and IL-5 in aerosols trapped by the polypropylene layer of a face mask with a low limit of detection of 10^{-2} pg·mL^{-1}. When the face masks were worn for 30 min by patients suffering from an acute COPD exacerbation episode our biosensors were able to detect higher inflammation in the airways in 100% of cases. When used to detect IL-5 in eosinophilic asthma patients with no exacerbation symptoms the proposed immunosensors identified high airways inflammation in 80% patients. The proposed biosensors enable detecting airways cytokines using a non-invasive sampling procedure. This could revolutionize the management of airways diseases by providing guidance for administering anti-inflammatory therapies.

ASSOCIATED CONTENT

Supporting Information

Materials (Section S1); Impact of polymer concentration on biosensor performance (Section S2); 3D device for face mask spraying (Section S3); Impact of face mask wearing time on colorimetric signals yielded by biosensors (Section S4); Feasibility study with a microarray disperser (Section S5); Correlation between blood cells counts and signals yielded by airway IL-5 immunosensors (Section S6).

AUTHOR INFORMATION

Corresponding Author

tonydelaricalab@gmail.com; roberto.delarica@ssib.es

Author Contributions

The manuscript was written through contributions of all authors. All authors have given approval to the final version of the manuscript.

DECLARATION OF COMPETING INTEREST

A patent application describing the method for storing nanoparticles in paper reservoirs has been filed (PCT/EP2020/075013).

ACKNOWLEDGMENT

R.R acknowledges funding from Instituto de Salud Carlos III through the project PI20/00538 (Co-funded by European Regional Development Fund/European Social Fund "A way to make Europe"/ "Investing in your future"). C.A. acknowledge INTRES: Invertir, investigar, innovar Junior fellowshipfrom IdISBa/Impost turisme sostenible/Agència d'Estratègia Turística de les Illes Balears/ Govern de les Illes Balears. A.V. acknowledges funding from the Instituto de Salud Carlos III (PFIS contract FI21/00167). We are grateful to C. Fernández-Sánchez and A. Baldi for facilitating the feasibility study with a microarray disperser (Section S5).

ABBREVIATIONS

AECOPD: acute exacerbation of chronic obstructive pulmonary disease

AuNPs: gold nanoparticles

BSA: bovine serum albumin

COPD: chronic obstructive pulmonary disease

CRP: C-reactive protein

EDC: 1-Ethyl-3-(3-dimethylaminopropyl) carbodiimide

IL-5: interleukin 5

IL-6: interleukin 6

MES: 2-(N-morpholino)ethanesulfonic acid

NHS: N-hydroxysuccinimide

PBS: Phosphate buffer saline

PBST: phosphate buffer saline tween

PEG: poly ethylene glycol

PSS: Poly styrene sulfonate sodium salt

RSD: relative standard deviation

RT: room temperature

SD: Standard deviation

REFERENCES

[1] Q. Li, Y. Xu, J. Qi, X. Zheng, S. Liu, D. Lin, L. Zhang, P. Liu, B. Li, L. Chen, A self-powered rotating paper-based analytical device for sensing of thrombin, Sens Actuators B Chem. 351 (2022). https://doi.org/10.1016/j.snb.2021.130917.

[2] H. Zhao, L. Dou, J. Ren, M. Cui, N. Li, X. Ji, X. Liu, C. Zhang, MOF-derived porous Co3O4 coupled with AuNPs and nucleic acids as electrocatalysis signal probe for sensitive electrochemical aptasensing of adenosine triphosphate, Sens Actuators B Chem. 362 (2022). https://doi.org/10.1016/j.snb.2022.131753.

[3] L. Zhang, W. Yin, Y. Tong, Y. Zhang, Y. Xu, S.Y. Liu, Z. Dai, X. Zou, Highly Efficient Isolation and Sensitive Detection of Small Extracellular Vesicles Using a Paper-Based Device, Anal Chem. 94 (2022) 10991–10999. https://doi.org/10.1021/acs.analchem.2c01378.

[4] A. Merkoçi, A. Sena-Torralba, R. Alvarez-Diduk, C. Parolo, H. Torné-Morató, A. Müller, Paper-based electrophoretic bioassay: Biosensing in whole blood operating via smartphone, Anal Chem. 93 (2021) 3112–3121. https://doi.org/10.1021/acs.analchem.0c04330.

[5] M.J. Arroyo, I. de Orbe-Payá, M. Ortega-Muñoz, J. Vilar-Tenorio, D. Gallego, G.J. Mohr, L.F. Capitán-Vallvey, M.M. Erenas, Capillary microfluidic platform for sulfite determination in wines, Sens Actuators B Chem. 359 (2022). https://doi.org/10.1016/j.snb.2022.131549.

[6] A. Vaquer, E. Barón, R. de La Rica, Dissolvable Polymer Valves for Sweat Chrono-Sampling in Wearable Paper-Based Analytical Devices, ACS Sens. 7 (2022) 488–494. https://doi.org/10.1021/acssensors.1c02244.

[7] X. Fu, B. Xia, B. Ji, S. Lei, Y. Zhou, Flow controllable three-dimensional paper-based microfluidic analytical devices fabricated by 3D printing technology, Anal Chim Acta. 1065 (2019) 64–70. https://doi.org/10.1016/j.aca.2019.02.046.

[8] C.C. Tseng, C. te Kung, R.F. Chen, M.H. Tsai, H.R. Chao, Y.N. Wang, L.M. Fu, Recent advances in microfluidic paper-based assay devices for diagnosis of human diseases using saliva, tears and sweat samples, Sens Actuators B Chem. 342 (2021). https://doi.org/10.1016/j.snb.2021.130078.

[9] S. Jahanshahi-Anbuhi, A. Henry, V. Leung, C. Sicard, K. Pennings, R. Pelton, J.D. Brennan, C.D.M. Filipe, Paper-based microfluidics with an erodible polymeric bridge giving controlled release and timed flow shutoff, Lab Chip. 14 (2014) 229–236. https://doi.org/10.1039/c3lc50762a.

[10] Y. Xia, C. Song, Y. Meng, P. Xue, A.J. deMello, Q. Gao, S. Stavrakis, S. Ma, X. Cao, An addressable electrowetting valve for centrifugal microfluidics, Sens Actuators B Chem. 369 (2022). https://doi.org/10.1016/j.snb.2022.132276.

[11] A. Alba-Patiño, C. Adrover-Jaume, R.D. la Rica, Nanoparticle Reservoirs for Paper-Only Immunosensors, ACS Sens. 5 (2020) 147–153. https://doi.org/10.1021/acssensors.9b01937.

[12] C.H. Huang, K.F. Lei, Quantitative study of tumor angiogenesis in three-dimensional matrigel barrier using electric impedance measurement technique, Sens Actuators B Chem. 370 (2022). https://doi.org/10.1016/j.snb.2022.132458.

[13] F. Criscuolo, I. Ny Hanitra, S. Aiassa, I. Taurino, N. Oliva, S. Carrara, G. de Micheli, Wearable multifunctional sweat-sensing system for efficient healthcare monitoring, Sens Actuators B Chem. 328 (2021). https://doi.org/10.1016/j.snb.2020.129017.

[14] A. Lamaoui, A. Karrat, A. Amine, Molecularly imprinted polymer integrated into paper-based analytical device for smartphone-based detection: Application for sulfamethoxazole, Sens Actuators B Chem. 368 (2022). https://doi.org/10.1016/j.snb.2022.132122.

[15] N. Nawaz, N.K. Abu Bakar, H.N. Muhammad Ekramul Mahmud, N.S. Jamaludin, Molecularly imprinted polymers-based DNA biosensors, Anal Biochem. 630 (2021). https://doi.org/10.1016/j.ab.2021.114328.

[16] M.M. González del Campo, A. Vaquer, R. de la Rica, Polymer Components for Paper-Based Analytical Devices, Adv Mater Technol. 7 (2022). https://doi.org/10.1002/admt.202200140.

[17] B. Kannan, S. Jahanshahi-Anbuhi, R.H. Pelton, Y. Li, C.D.M. Filipe, J.D. Brennan, Printed Paper Sensors for Serum Lactate Dehydrogenase using Pullulan-Based Inks to Immobilize Reagents, Anal Chem. 87 (2015) 9288–9293. https://doi.org/10.1021/acs.analchem.5b01923.

[18] M. del M. González del Campo, A. Alba-Patiño, C. Palomino, M. Bauzá, E. Rojo-Molinero, A. Oliver, G. Turnes, R. de la Rica, Boosting the sensitivity of paper-based biosensors with polymeric water-soluble reservoirs, Sens Actuators B Chem. 354 (2022). https://doi.org/10.1016/j.snb.2021.131214.

[19] P. He, B. Derby, Controlling Coffee Ring Formation during Drying of Inkjet Printed 2D Inks, Adv Mater Interfaces. 4 (2017). https://doi.org/10.1002/admi.201700944.

[20] D. Mampallil, H.B. Eral, A review on suppression and utilization of the coffee-ring effect, Adv Colloid Interface Sci. 252 (2018) 38–54. https://doi.org/10.1016/j.cis.2017.12.008.

[21] A. Turkeli, O. Yilmaz, F. Taneli, G.D. Horasan, E.T. Kanik, M. Kizilkaya, C. Gozukara, H. Yuksel, IL-5, IL-8 and MMP -9 levels in exhaled breath condensate of atopic and nonatopic asthmatic children, Respir Med. 109 (2015) 680–688. https://doi.org/10.1016/j.rmed.2015.04.004.

[22] E. Bucchioni, S.A. Kharitonov, L. Allegra, P.J. Barnes, High levels of interleukin-6 in the exhaled breath condensate of patients with COPD, Respir Med. 97 (2003) 1299–1302. https://doi.org/10.1016/j.rmed.2003.07.008.

[23] C. Adrover-Jaume, A. Alba-Patiño, A. Clemente, G. Santopolo, A. Vaquer, S.M. Russell, E. Barón, M. del M. González del Campo, J.M. Ferrer, M. Berman-Riu, M. García-Gasalla, M. Aranda, M. Borges, R. de la Rica, Paper biosensors for detecting elevated IL-6 levels in blood and respiratory samples from COVID-19 patients, Sens Actuators B Chem. 330 (2021). https://doi.org/10.1016/j.snb.2020.129333.

[24] A. Alba-Patiño, S.M. Russell, M. Borges, N. Pazos-Pérez, R.A. Álvarez-Puebla, R. de La Rica, Nanoparticle-based mobile biosensors for the rapid detection of sepsis biomarkers in whole blood, Nanoscale Adv. 2 (2020) 1253–1260. https://doi.org/10.1039/d0na00026d.

[25] K. Maejima, S. Tomikawa, K. Suzuki, D. Citterio, Inkjet printing: An integrated and green chemical approach to microfluidic paper-based analytical devices, RSC Adv. 3 (2013) 9258–9263. https://doi.org/10.1039/c3ra40828k.

[26] C. Seo, D. Jang, J. Chae, S. Shin, Altering the coffee-ring effect by adding a surfactant-like viscous polymer solution, Sci Rep. 7 (2017). https://doi.org/10.1038/s41598-017-00497-x.

[27] H. Huang, X. Huang, K. Zeng, F. Deng, C. Lin, W. Huang, Interleukin-6 is a strong predictor of the frequency of copd exacerbation within 1 year, International Journal of COPD. 16 (2021) 2945–2951. https://doi.org/10.2147/COPD.S332505.

[28] A. Bhowmik, T.A.R. Seemungal, R.J. Sapsford, J.A. Wedzicha, Relation of sputum inflammatory markers to symptoms and lung function changes in COPD exacerbations, Thorax. 55 (2000) 114–120. https://doi.org/10.1136/thorax.55.2.114.

[29] S.T. Holgate, Pathogenesis of asthma., Clin Exp Allergy. 38 (2008) 872–897. https://doi.org/10.1111/j.1365-2222.2008.02971.x.

[30] Z.J. Amini-Vaughan, M. Martinez-Moczygemba, D.P. Huston, Therapeutic strategies for harnessing human eosinophils in allergic inflammation, hypereosinophilic disorders, and cancer, Curr Allergy Asthma Rep. 12 (2012) 402–412. https://doi.org/10.1007/s11882-012-0290-3.

[31] A.W. Collinsworth, A.L. Masica, R. Kudyakov, V. Bayer, M.W. Millard, A. Shaikh, Retrospective observational study of asthma and chronic obstructive pulmonary disease prevalence and associated healthcare resource utilization in a large, integrated healthcare system, Baylor University Medical Center Proceedings. 35 (2022) 737–745. https://doi.org/10.1080/08998280.2022.2096370.

Graphical Abstract